Genia Versha Fernanda

Modelling Ocean Depths from Half-Space Cooling

Introduction

The profound relationship between temperature and density in the oceanic lithosphere significantly affects Earth's heat dissipation, particularly through plate creation at ridges. As hot rock emerges at the ridge, cools, and reaches the ocean, changes in density occur, leading to subsequent subsidence (Crosby et al., 2006). Understanding this temperature-density connection elucidates variations in depth concerning seafloor age (Carlson & Johnson, 1994). Unlike continental lithosphere, the oceanic lithosphere presents a simple mechanism for finding dynamic topography, wherein depth evolution correlates with plate cooling and thickening (McKenzie, 1967; Hoggard et al., 2017).

As the lithosphere cools and thickens indefinitely as a function of age, we can define its connection by using a half-space model that involves conductive cooling of a semi-infinite mantle half-space with a fixed temperature along the surface and depth at the ridge axis (Turcotte & Oxburgh, 1969). This primary thermal model for the oceanic lithosphere posits a half-space initially at a constant temperature, cooling from the top through conduction, setting up a direct correlation between temperature and density. Seafloor regions are strategically chosen to eliminate the influence of thermal rejuvenation, flexure from volcanic loads or subduction, and the presence of seamounts (Crosby et al., 2006). Davis and Lister (1974) demonstrated a significant concordance between the half-space cooling model and the mean depth of the central-eastern Pacific, especially within the 80 million years timeframe.

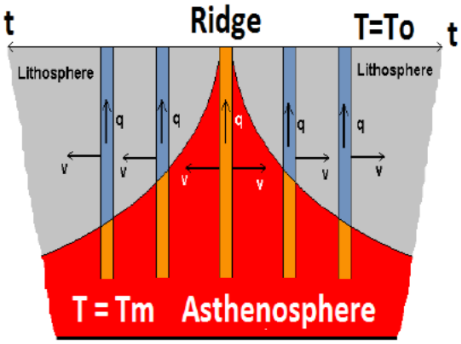

In the Half-Space Cooling (HSC) model, the lithosphere acts as the boundary layer of the mantle convection system, with its thickness increasing continuously as it moves away from the *upwelling* limb. The model assumes that the lithosphere's thickness remains consistently much less than that of the underlying magma-rich asthenosphere mantle, allowing the latter to be treated as a semi-infinite half-space for studying the cooling history of the overlying boundary layer (Cardoso and Hamza, 2011).

Figure 1. Schematic illustration of the geometry adopted in the half-space cooling (HSC) model; the principle of isostasy dictates that the ocean deepens with age to counterbalance thermal contraction in the lithosphere.

Datasets used in the analysis were obtained from Smith & Sandwell (1997) for the bathymetry and Müller et al. (2018) for the crustal age map. The predicted bathymetry was extracted from spatially binned ship track data, using tension splines (T = 0 and T = 1) and differing it by 21 and 36 m, indicating consistent data coverage at the hundreds of kilometres scale. Depth anomalies on young seafloor relate to seismic velocity patterns, suggesting lithospheric and sub-lithospheric density variations, with shallow depths corresponding to increased seamount volcanism, possibly associated with hot spots (Smith & Sandwell, 1997). Concerning the crustal age, GPlates (GPROJ) data provides a versatile plate motion model spanning the last 410 million years. The software also facilitates the partitioning of the Earth's surface into tectonic elements. For continents, it offers outlines, paleomagnetic data, and continent-ocean boundaries, while oceanic crust data includes fabric, age isochrons, and mid-oceanic ridges (Matthews et al., 2011; Müller, Seton, et al., 2016, Müller et al. 2018). Furthermore, it allows flexible visualization of oceanic basin evolution and provides bundled time-dependent raster like age-coded subducted slabs (Müller et al., 2018).

Methodology

Table 1. Constants and parameters for half-space cooling boundary conditions and isostatic modelling.

Parameter	Symbol	Value
Temperature at the Ocean floor	T_S	0 ° C
Temperature of molten Lithosphere	T_m	1300 °C
Density of mantle (molten oceanic lithosphere)	ρ_m	3.25 g.cm^3
Density of water	ρ_w	1000 kg.m^{-3}
Specific heat capacity of silicate rocks	C_p	710 J.kg^{-1}. K^{-1}
Thermal conductivity of silicate rocks	k	2,3,4 W.m^{-1}. K^{-1}
Coefficient of thermal expansion for peridotite	α	2.4 x 10^{-5} K^{-1}
Typical depth to the ocean floor at East Pacific Rise	h_{ridge}	2.5 km
Maximum age of Pacific oceanic crust	t	200 Myr
Initial column of thickness at Temperature=T_m and ρ_m at t=0	z_L	250 km

A. Generate Half-Space Cooling Model

First step to generate the Half-space cooling model is generating 2D temperature arrays in respect of each age and depth. In this model, it's important to note that density is **assumed to be temperature-dependent**, a condition that is nearly impossible in the real world. In the oceanic lithospheres, it is known that the crust composed of different materials which has different composition, permeability, and other physical properties that play significant roles in determining density. Therefore, simplifying density as solely dependent on temperature oversimplifies the nature of density variations in real-world materials.

The temperature within the rock column is a function of depth and time ($T = T(z,t)$), and the **density of the cooling rock column is exclusively determined by only its temperature** and varies with depth and time ($\rho(z,t)$), to be: $\rho(z, t) = \rho_m + \alpha\rho_m(T_m - T(z,t))$.

Regarding the topographic behaviour, Sclater and Francheteau; Davis and Lister (1973) provide the comprehensive equation for a vertical boundary with a **constant initial temperature**, incorporating temperature dependence into thermal parameters and phase changes:

$$\rho CpU\frac{\partial T}{\partial x} = K\left(\frac{\partial^2 T}{\partial x^2} + \frac{\partial^2 T}{\partial z^2}\right) + H \qquad \rightarrow \qquad \frac{l}{l_0}\frac{\partial T}{\partial x} = \frac{\partial^2 T}{\partial x^2} + \frac{\partial^2 T}{\partial z^2}$$

The **isostatically compensated topographic height, at constant initial density ρ_0**, for initial column $\rho(z, 0) = \rho m$ can be defined by using:

$$\int_0^{z_L}(\rho(z,t) - \rho_m)dz \qquad \rightarrow \qquad \left(\frac{\sum_{z=0}^{z_L}\rho(z,t)}{n} - \rho_m\right)z_L$$

The temperature at any point within the column of rock T is a function of depth from the surface in metres and time t in seconds: $T = T(z, t)$. We can find the temperature $T(z, t)$ with the solution to the one-dimensional heat conduction or diffusion equation:

$\frac{T(z,t)-T_S}{T_m-T_S} = \text{erf}\left(\frac{z}{2\sqrt{\kappa t}}\right)$; with the thermal diffusivity $\kappa = \frac{k}{\rho C_p}$

B. Calculate Density and Water Thickness

Further, **hydrostatic equilibrium** is achieved when the total hydrostatic pressure of a column with a thickness of ($z_L + h_w$) at the ridge axis equals the pressure of a column with the same thickness at any age/distance from the ridge axis, providing insights into lateral variations in ocean floor depth. Utilizing

this information, an expression is defined that considers the densities and thicknesses of the initial column, the cooled column at time t and the thickness of water that sits above the cooled column h_w:

$$\rho_m(z_L + h_w) = h_w\rho_w + \int_0^{z_L} \rho(z,t)dz$$

$$h_w(\rho_w - \rho_m) = \int_0^{z_L} (\rho(z,t) - \rho_m)dz = 0$$

And then reorder the equation to obtain the thickness of water:

$$h_w = \int_0^{z_L} \frac{(\rho_m - \rho(z,t))}{\rho_m + \rho_w} dz = 0$$

Besides the assumptions for solving equations, parameter values, including thermal conductivity, thermal expansion coefficient, and specific heat capacity ranges, are determined from past experiments, considering factors like pressure-dependence and anisotropy. Most thermal models of the Earth's lithosphere assume a constant *k* value (typically ranging from 2 to 5 W m-1 K-1) due to uncertainties associated with conventional contact methods at high temperatures (Whittington et al., 2009).

C. Assess Misfit with Real-world Data

Next **assumption was made for the isostatic correction**, which we can do by **removing the seamounts**. It can be done by adding the ridge depth of 2500 meters to the obtained subsidence, where the ridge depth is determined such that the misfit between the predicted and observed seafloor depths becomes a minimum. The removal of the surface features like seamount reduces the deviations of topography moderately. The value of 2500 is based on the average value of the observation's depth. Beside seamount, there are other topographic measurements that might be needed to get eliminated, like plateaus, flexural moats, and major fracture zones.

Results

A. Half-Scale Cooling Model of Depth

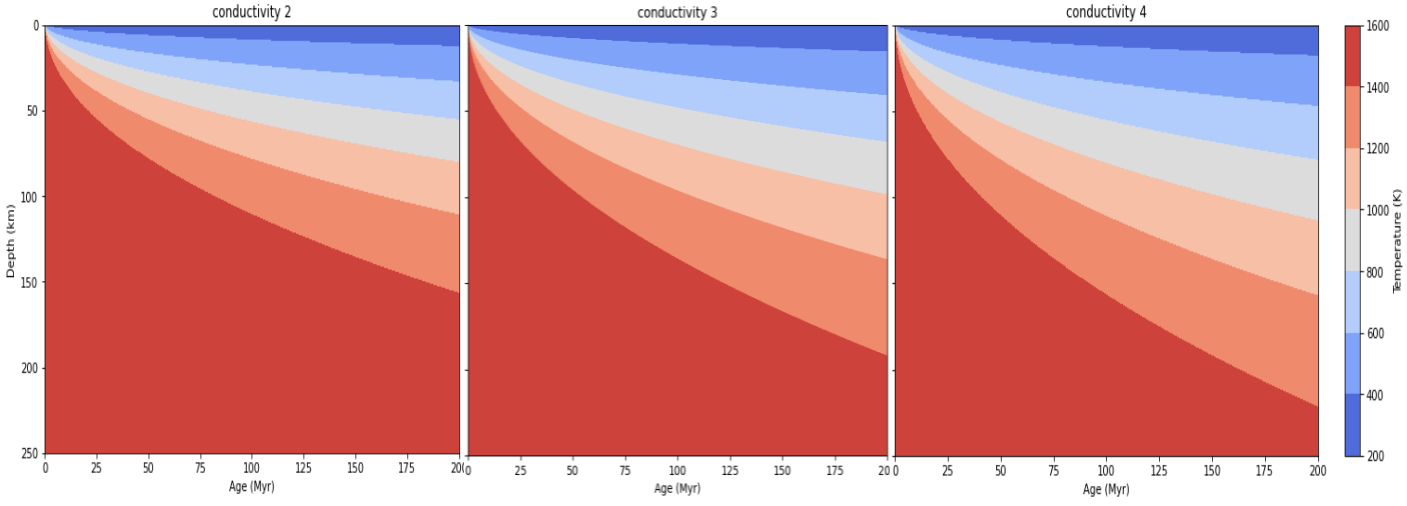

Figure 2. Comparison of *isotherms* as a function of age to three different thermal conductivity (*k*) that vary with age, highlighting the consistent cooling of the lithosphere. Depths are presented relative to the crestal depth, with a scale in 50 km increments. The depicted subsidence rates are indicative of the cooling and thickening of the Earth's lithosphere, as reflected in the temperature values. Notably, the subsidence rate shows a linear increase with thermal conductivity, progressing by 30 km.

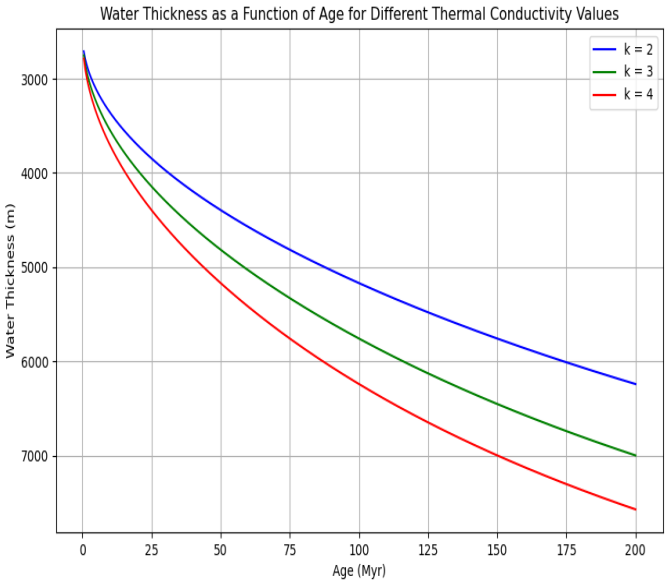

Figure 3. Displayed are models depicting water thickness utilizing the half-space cooling model with three varied thermal parameters. The graph illustrates water thickness as a function of seafloor age. The lowest thermal conductivity (*k*) corresponds to the minimum water thickness. Its graph mirrors the isotherm plot, given that the modeled depth is determined by temperature-dependent density value. Specifically, for k=4, the water thickness reaches a depth of nearly 8000m, surpassing other k values.

B. Misfits, Model Fit Dynamics, and Age-Dependent Trends in Oceanic Depths

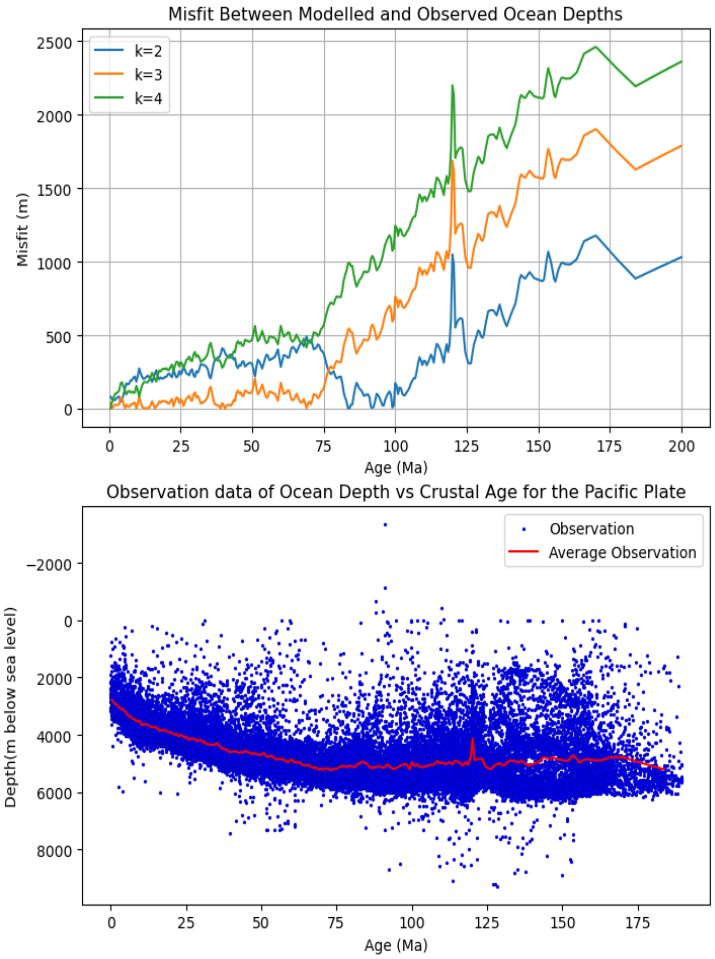

Figure 4a) Misfit comparison between half-scale cooling model in Pacific plate with the depth observation data, with dynamic topography subtracted (h_{ridge}=2500 m, based on the average observation depth), the best fit arises from the model with *k=3*. This model exhibits a value closer to 0, indicating a satisfactory fit, though it begins to deteriorate around 75 Myr age. However, for ages beyond 75 Myr age, the best-fit model poorly aligns with the depth-age variation **(Top)**.; **4b)** Average observation of depth for a range of sorted age data. Data and models for ocean depth as a function of age. Depths are an average of Pacific Ocean ranging from 60°N-60°S, 130°E-100°W. The data are averaged in 0.5 Myr bins and one standard deviation about the mean value for each is shown by the red line **(Bottom)**.

C. Pacific Plate Dynamics: Topography, Age, and Model-Reality Discrepancies Unveiled

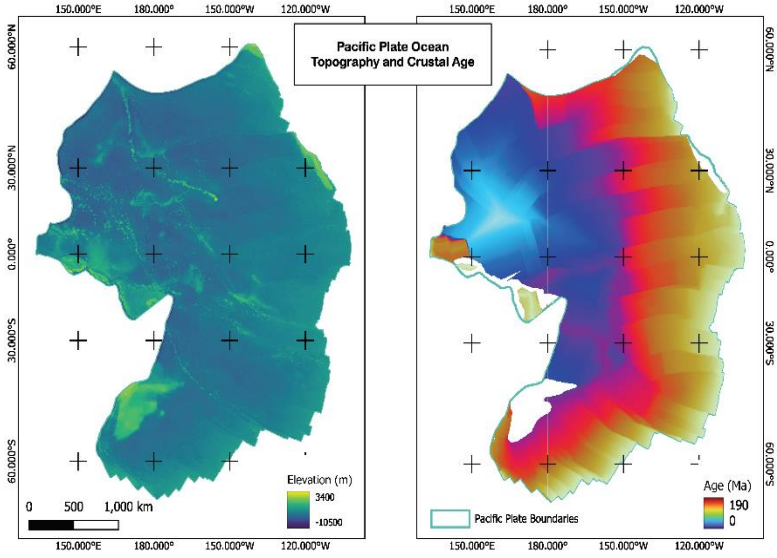

Figure 5. Bathymetry **(left)** and crustal age map **(right)** compiled from diverse datasets for the Pacific plate. The apparent thermal age for the Pacific is derived from GPlates (Müller et al., 2018). The topographic maps for the Pacific are shown before isostatic corrections. The Crustal Age grid, containing data only for ocean floor regions, results in negative elevation values that need adjustment. The maximum age of crust in the Pacific Plate is 200 Myr.

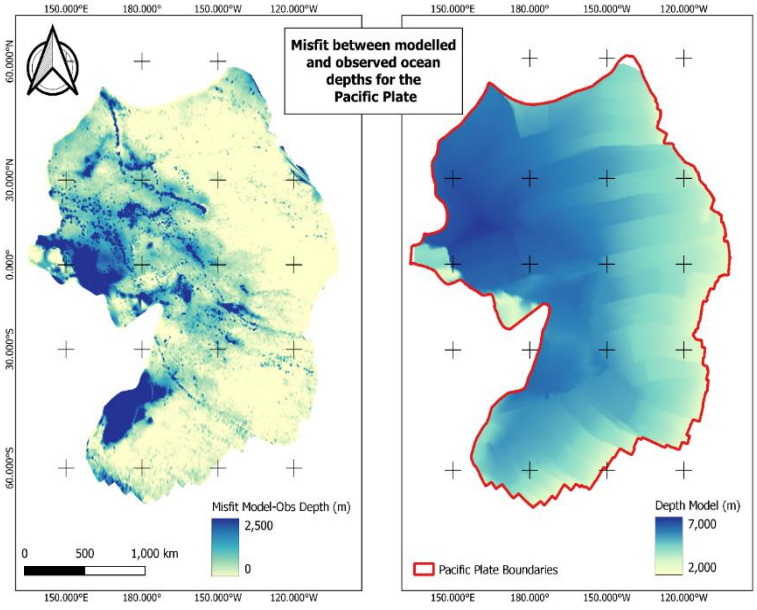

Figure 6. Misfit **(left)** and modeled depth as a function of crustal age **(right)**. The effective fit is evident, particularly for ages less than 75 Myr, depicted by the light colour scale on the map. This alignment is also apparent in the depth model map, illustrating shallower depths for younger ages (based on **Figure 5**) in comparison to the older Pacific crust. The depth model is derived through interpolation from the age data. This corresponds with the contour plot of water thickness, highlighting that *k=3* results in shallower depths compared to *k=2*.

Discussions

A. Decoding Lithospheric Dynamics: Age-Dependent Effects and Thermal Relations

In the result shown in **Figure 2** and **Figure 3**, the age data is organized into 25-Myr age intervals from 0 to 200-Myr, reveals a thermal diffusivity value of 1.733e-06 m^2/s. Furthermore, the temperature structures within oceanic plates, calculated from models assuming constant initial temperature during lithosphere creation (which was defined by using a fixed value for the mantle and surface temperature) and subsequent age-dependent cooling, establish a marked contrast between the Earth's young oceanic plates and the ancient continental crust, formed over 3 billion years ago (Hawkesworth et al. 2019). This distinction is integral, given the consistent subduction of oceanic crust along continental and oceanic arcs. Additionally, the exploration of thermal conductivity in **Figure 2** underscores its linear relationship with density, offering insights into how heat is conducted through geological materials and influencing temperature distribution within the rock column.

The graph highlights the nuanced impact of varying thermal conductivity (*k*), on the subsidence behaviour of a cooling column of rock over time (**Figure 2**). Furthermore, it is noticeable that the decrease in k with rising temperature contributes to a lower central plate temperature. Overall, the findings emphasize the nuanced interplay of thermal conductivity, specific heat capacity, and density, particularly within the k=2 to k=4 range, with the intermediate value of k=3 appearing closer to the actual physical conditions influencing the depth observations data (**Figure 3**).

The relationship between thermal conductivity and density plays a pivotal role in determining the required thickness of water for a cooling rock column. Specifically, as thermal conductivity increases or density decreases, the thermal diffusivity of the material rises. The simplistic cooling oceanic plate model assumes constant thermal conductivity, whereas the actual decrease in thermal conductivity with rising temperature causes the central plate temperature to be less than the model's prediction. Furthermore, beneath shields, Moho temperature is primarily controlled by crustal thickness and heat generation rate, challenging conventional assumptions, and indicating higher Moho temperatures than previously believed.

B. Model-Reality Mismatch in Ocean Depths

In **Figure 4a**, the misfit comparison between the half-scale cooling model in the Pacific plate and observed depth data with dynamic topography subtracted by h_{ridge} = 2500 m reveals critical insights into plate cooling parameters. The h_{ridge} value is defined by using the average value of the depth observation from **Figure 4b**, which showing the range value of 2000-3000 m. As highlighted by McKenzie et al. (2005), the temperature-dependence of thermal conductivity significantly influences half-space model, impacting the cooling and thickening of the oceanic lithosphere. This dynamic interplay controls both bathymetry and heat flow, offering valuable insights into diverse geological processes. Further, substantial internal heating and small-scale convection contribute to the seafloor depth (Huang and Zhong, 2005). **Figure 4a** and **4b** illustrates *k*=3 provides a satisfactory fit, aligning well with observations up to 75 Myr age but encounters challenges beyond this threshold. This breakdown is consistent with Schroeder's (1984) argument regarding the limitations of the half-space model in the entire Pacific basin beyond 80 Ma, influenced by hot spots or hot spot tracks.

Fixing the misfit and improving the model accuracy, incorporating additional factors such as pressure dependence of thermal properties becomes crucial. Richards et al. (2018) propose considering pressure dependence alongside temperature and lithology-dependence, which may result in the variability of thermal conductivity and thermal expansion coefficient. Additionally, exploring parameters like radiative thermal conductivity, known for its lower grain size dependence, could further refine the model's depth predictions. These adjustments aim to refine our understanding of plate cooling dynamics and improve the model's alignment with observed data.

C. Exploring Factors Influencing Model-Reality Discrepancies in Pacific Plate Modeling

Based on **Figure 5** and **Figure 6**, notably the Pacific Ocean lithosphere older than 80 Ma is within the average radius to which hot spots occurred. The model in this research knowledges three factors not considered: the pressure-dependence of the thermal expansion coefficient (Grose & Afonso, 2013), incomplete thermal contraction owing to the high viscosity of the oceanic plate (Korenaga, 2007), and inaccuracies in mineral physics approximations for modeling the thermal expansivity coefficient (Grose & Afonso, 2013). The neglection of these factors could lead to an inefficiency of the model for older crustal ages. Another possible reason of the model is more effective for young ages is because the oceanic lithosphere’s behaviour often dominated by more straightforward processes during its initial formation and earth cooling stages.

The model focuses solely on depth variation due to cooling lithosphere, excluding the potential impact of large- and small-scale convection, mantle temperature variations, and phase changes, with no incorporation of time-dependent effects beyond cooling, such as the proposed *Cretaceous superplume* (Stein & Stein, 1992). Recognizing that the density-temperature relationship in the model is an oversimplification, as oceanic crustal density is influenced by various factors, including different crustal materials impacting heat transfer and subsequent depth variations. The misfit in older crustal ages may stem from the bottom boundary condition's impact on integrated temperature at ages younger than its surface-reaching effect (**Figure 6**). Additionally, hydrothermal circulation and fluid flow play roles, affecting heat transfer fraction and lowering temperatures in shallow depths of young lithosphere. Seafloor topography is deemed a robust constraint, aligning with the subsidence of young-age seafloor predicted by simple half-space cooling models (Grose, 2012).

References

Carlson, R. L., and H. P. Johnson (1994), On modeling the thermal evolution of the oceanic upper mantle: An assessment of the cooling plate model, J. Geophys. Res., 99, 3201–3214.

Carslaw, H. S. and Jaeger, J.C. (1959), Conduction of Heat in Solids, Oxford University Press, USA, 2nd Ed.

Crosby, A. G., D. McKenzie, and J. G. Sclater (2006), The relationship between depth, age, and gravity in the oceans, Geophys. J. Int., 166, 553–573.

Davis, E. E., and C. R. B. Lister (1974), Fundamentals of ridge crest topography, Earth Planet. Sci. Lett., 21, 405.

Grose, C. J. (2012), Properties of oceanic lithosphere: revised plate model predictions, Earth Planet. Sci. Lett., 333–334, 250–264.

Grose, C. J. and Afonso, J. C. (2013), Comprehensive plate models for the thermal evolution of oceanic lithosphere, Geochem. Geophy. Geosy., 14, 3751–3778.

Hawkesworth, C., P.A. Cawood, B. Dhuime. (2019), Rates of generation and growth of the continental crust, Geosci. Front., 10, 165-173.

Huang, J., and S. Zhong (2005), Sublithospheric small-scale convection and its implications for residual topography at old ocean basins and the plate model, J. Geophys. Res., 110, B05404.

Korenaga, J. (2007a), Effective thermal expansivity of Maxwellian oceanic lithosphere, Earth Planet. Sci. Lett., 257, 343–349.

Lister, C. R. B., J. G. Sclater, E. E. Davis, H. Villinger, and S. Nagihara (1990), Heat flow maintained in ocean basins of great age: Investigations in the north-equatorial west Pacific, Geophys. J. Int., 102, 603–630.

McKenzie, D. P. (1967), Some remarks on heat flow and gravity anomalies, J. Geophys. Res., 72, 6261–6273.

McKenzie, D., J. Jackson, and K. Priestley (2005), Thermal structure of oceanic and continental lithosphere, Earth. Planet. Sci. Lett., 233, 337–349.

Müller, R. D., Cannon, J., Qin, X., Watson, R. J., Gurnis, M., Williams, S., Pfaffelmoser, T., Seton, M., J. Russell, S. H., & Zahirovic, S. (2018), GPlates: Building a Virtual Earth Through Deep Time. Geochemistry, Geophysics, Geosystems, 19(7), 2243-2261.

Richards, F. D., Hoggard, M. J., Cowton, L. R., & White, N. J. (2018), Reassessing the thermal structure of oceanic lithosphere with revised global inventories of basement depths and heat flow measurements. Journal of Geophysical Research: Solid Earth, 123, 9136–9161.

Schroeder, W. (1984), The empirical age-depth relation and depth anomalies in the Pacific Ocean basin, J. Geophys. Res., 89.

Smith, W. H. F., and D. T. Sandwell (1997), Global Sea floor topography from satellite altimetry and ship depth soundings, Science, 277, 1956–1962.

Stein, C. Stein, S. (1992), A model for the global variation in oceanic depth and heat flow with lithospheric age. Nature, 359:123–129.

Turcotte, D., and E. Oxburgh (1967), Finite amplitude convective cells and continental drift, J. Fluid Mech., 29.

Von Herzen, R., E. E. Davis, A. T. Fisher, C. A. Stein, and H. N. Pollack (2005), Comments on ‘‘Earth’s heat flux revised and linked to chemistry’’ by A.M. Hoffmeister and R.E. Criss, Tectonophysics, 409, 193–198.

Whittington, A., Hofmeister, A. & Nabelek, P. (2009), Temperature-dependent thermal diffusivity of the Earth’s crust and implications for magmatism. Nature, 458, 319–321.